

Vision-Based Multi-Task Manipulation for Inexpensive Robots Using End-To-End Learning from Demonstration

Rouhollah Rahmatizadeh, Pooya Abolghasemi, Ladislau Bölöni,
Department of Computer Science
University of Central Florida, United States
{rrahmati, pooya.abolghasemi, lboloni}@cs.ucf.edu

Sergey Levine
University of California Berkeley, United States
svlevine@eecs.berkeley.edu

Abstract: In this paper, we propose a multi-task learning from demonstration method that works using raw images as input to autonomously accomplish a wide variety of tasks in the real world using a low-cost robotic arm. The controller is a single recurrent neural network that can generate robot arm trajectories to perform different manipulation tasks. In order to learn complex skills from relatively few demonstrations, we share parameters across different tasks. Our network also combines VAE-GAN-based reconstruction with autoregressive multimodal action prediction for improved data efficiency. Our results show that weight sharing and reconstruction substantially improve generalization and robustness, and that training on multiple tasks simultaneously greatly improves the success rate on all of the tasks. Our experiments, performed on a real-world low-cost Lynxmotion arm, illustrate a variety of picking and placing tasks, as well as non-prehensile manipulation.

Keywords: Multi-task learning, Robot manipulation, Affordable assistive robotics

1 Introduction

Autonomous open-world execution of a wide variety of manipulation skills is an important goal of robotic learning. Open-world manipulation must handle complex perception and a multitude of tasks. Of particular interest in this work is the performance of activities of daily living (ADLs): everyday tasks that able-bodied individuals perform with ease, but that can be a major challenge for a disabled or elderly person. Assistive robots performing ADLs need to operate in the uncontrolled environment of the user’s home. To achieve maximum social impact, it would be desirable to develop perception and control methods that can use low-cost, imprecise hardware and readily-available sensory inputs such as camera images.

One approach to make robots autonomous is to hand-engineer a controller that is specific to a certain task. However, in the open-world settings we considered, hand-engineering a robust and resilient vision-based control strategy is exceptionally difficult. Learning from demonstration (LfD) allows humans to demonstrate different tasks to the robot without having any knowledge about the robot’s control or programming model. Because LfD can be performed using standard, efficient supervised learning methods, it requires orders of magnitude fewer interactions than reinforcement learning methods that learn from scratch. However, as the demonstrations need to be performed by humans, it is important to reduce their number as much as possible. In this paper, we propose an efficient learning approach that combines data from multiple tasks, as well as an auxiliary reconstruction loss, to learn a single multi-task recurrent neural network policy from a tractable number of demon-

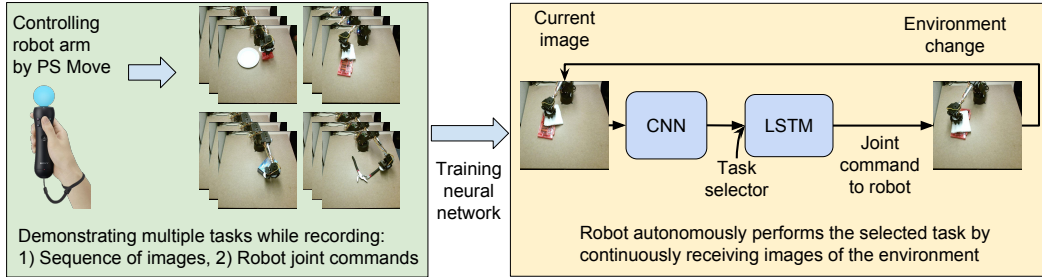


Figure 1: An overview of our approach to multi-task learning

strations. The policy takes as input images of the environment and a task selector one-hot vector, and predicts the joints of the robot in the next time-step.

Recurrent neural networks are powerful models for learning sequential data, such as robot movement trajectories. However, they need relatively large numbers of training samples, which is not currently easy to obtain in the robotics domains. In this work, we use a single neural network and train it with all the data that we have gathered from multiple related tasks. This way, the common patterns among different tasks can be learned more easily since there is more data that contains those patterns. In addition, we use an autoregressive estimator to improve statistical efficiency and model multi-modal distributions in the actions. By sharing parameters across tasks, using an efficient autoregressive estimator, and regularizing via image reconstruction, we can improve generalization and success rates using a tractable number of demonstrations. An overview of our approach is illustrated in Figure 1. Our experimental results show that even with imprecise demonstrations and a low-cost manipulator, our method can perform a variety of manipulation tasks, including picking and placing and non-prehensile manipulation, can correct its mistakes, attempt tasks multiple times, and achieve high success rates.

The primary contributions of this paper are as follows: 1) We show that direct behavioral cloning enables the robot to learn vision-based control policies on an imprecise, low-cost robotic platform. 2) We describe a novel model architecture that combines image reconstruction for regularization with autoregressive action prediction for sample-efficient learning of multimodal action distributions. 3) We show that training a single network simultaneously on multiple tasks improves performance across tasks.

2 Related Work

Two main approaches to learning robot behaviours are Learning from Demonstration (LfD) and Reinforcement Learning (RL). Most LfD methods assume access to a reasonable perception system to localize objects in the environment. However, LfD for open-world manipulation, where the robot might encounter a variety of objects and scenes, is challenging: we must pick how to represent the world in a fixed-size representation, accurately localize objects, and handle perception errors. In this work, we instead perform LfD from raw image observations, which removes the need for a separate perception system and allows us to train a single policy for manipulating a variety of objects. LfD has achieved many successful applications such as autonomous helicopter maneuvers [1], playing table tennis [6], object manipulation [28], and making coffee [35]. This success comes at the expense of user’s time to demonstrate the tasks to the robot. On the other hand, RL approaches allow the robot to acquire different skills by itself [17, 29].

Both RL and LfD approaches need relatively large number of examples for training. Therefore, researchers have tried different approaches to reduce the number of required examples, such as transfer learning [37, 18, 33, 24]. An early work considered learning a neural network policy on multiple related tasks with backpropagation [7]. It is possible to learn this kind of policies by considering both the state and the task as input to the policy [8]. Neural networks policies can be decomposed to different modules where there are some task-specific modules and some robot-specific modules [9]. It is also shown that sharing the parameters of a neural network among different tasks not only improves the results, but also it is even better to train the model using the data of multiple related tasks instead of using the same amount of data from the original task [31].

Deep neural networks have been successfully used to map a robot’s visual input to control commands [21, 30, 2, 22, 23]. In this paper, we propose an end-to-end deep neural network architecture that can learn multiple tasks more efficiently and with a higher success rate than a single-task network.

3 Learning the Multi-Task Controller

The overall flow of our method consists of (1) collecting a set of demonstrations for multiple tasks, (2) training a single deep recurrent neural network to emulate the user’s behavior on all of the tasks simultaneously and (3) deploying the system in the real world using raw camera perception to perform the tasks.

3.1 Task Demonstration and Data Collection

To collect demonstrations, we needed to enable human control of the robot using a low-cost and intuitive teleoperation system. Low-cost robots do not have zero-gravity modes suitable for demonstration. Remote control techniques based on mouse or keyboard were found to be not intuitive for an assistive robotics scenario. The technique we used is for the robot end-effector to follow the user’s hand, who can then use natural movements to demonstrate the task. We found two solutions for capturing the position and orientation of the hand: (a) using a Leap Motion controller and a “naked” hand, and (b) using a Playstation Move controller. More details of the demonstration procedure are explained in Appendix A.

3.2 Neural Network Architecture

Our network architecture is illustrated in Figure 2. Convolutional layers augmented with batch normalization [13] process the input images and map them to a low dimensional feature representation according to the VAE-GAN approach [20]. VAE-GAN tries to encode input images based on the idea of Variational Autoencoders [15] and reconstruct realistic images based on the idea of Generative Adversarial Networks [10]. In VAE-GAN approach, a discriminator is added to the generator to discriminate the reconstructed images with the real images. However, instead of directly comparing the image pixels that causes uncertainty to appear in the form of blurriness, the extracted features of the real and reconstructed images after the third convolutional layer of the discriminator are compared together. On the bottom half of the Figure 2, we have a controller network where the extracted visual features are combined with a task selector one-hot vector and fed into 3 layers of layer normalized [3] LSTM [12] to generate joint commands to control the robot.

Most manipulation tasks can be solved in several distinct ways, and human demonstrators are often inconsistent of which solution they choose, even for the same task. A unimodal predictor, such as a Gaussian distribution, will average out dissimilar motions. By using a multi-modal predictor, we can capture different modes in the demonstrations without excessive averaging. However, simple multi-modal distributions such as mixtures of Gaussians [5] provide a number of modes that scales linearly with the number of parameters. Instead, we are using a multi-modal autoregressive estimator similar to Neural Autoregressive Distribution Estimator (NADE) [19], to increase the number of modes the model can represent exponentially with the number of steps of the autoregressive model. While autoregressive estimators usually discretize the output, we use mixture of Gaussians to predict the entire probability distribution of the output, providing a rich and expressive class of distributions.

A closer look at the architecture shows that we have a VAE-GAN autoencoder that shares its encoder with the visual feature extractor of a controller network that sends commands to the robot. The encoder tries to fully reconstruct the images while the controller network will try to focus on some relevant features from the image such as the pose of the gripper and relevant objects. This competition/collaboration between these two networks will result in a more regularized visual feature extractor. This idea is similar to the semi-supervised learning with generative models [16] where they use a generative model via the VAE decoder and discriminative training via the action branch to improve sample efficiency. However, in contrast to this work, we observe an improvement in generalization simply from including the reconstruction objective, without including any additional unlabeled data.

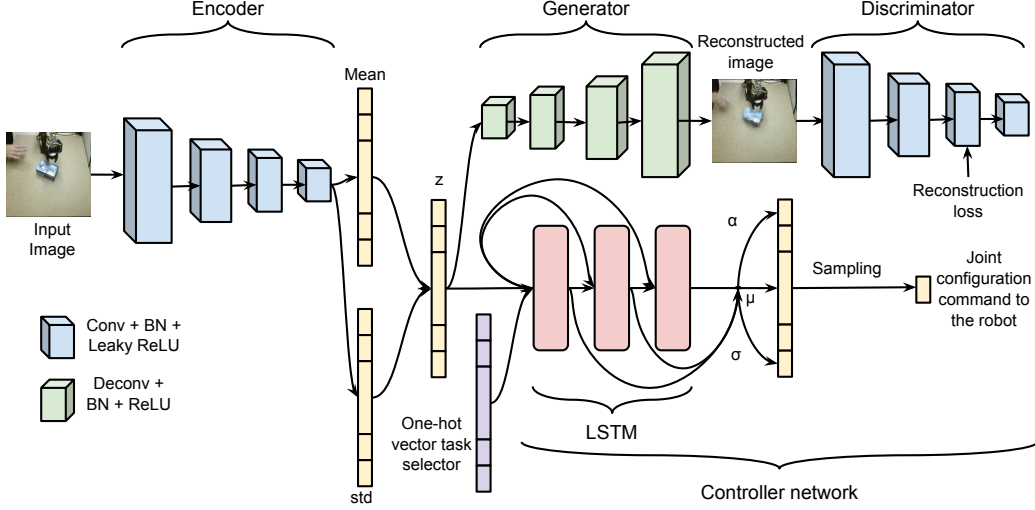


Figure 2: Our proposed architecture for multi-task robot manipulation learning. The neural network consists of a controller network that outputs joint commands based on a multi-modal autoregressive estimator and a VAE-GAN autoencoder that reconstructs the input image. The encoder is shared between the VAE-GAN autoencoder and the controller network and extracts some shared features that will be used for two tasks (reconstruction and controlling the robot).

Note that the extracted features from the encoder are in the form of a probability distribution that is encouraged to be close to the unit Gaussian by a KL-divergence penalty in the loss function. The noise in the LSTM input caused by sampling from the encoded latent features helps to regularize the LSTM. In addition, we use dropout [34] with a probability of 0.5 to further avoid overfitting.

3.3 Training the Network

The error signal that is used to train the network using back-propagation is based on the idea of Mixture Density Networks (MDN) [5]. In this approach, the output of the LSTM network is used to predict the parameters of a multi-modal mixture distribution. However, we do not predict all the outputs (joint configurations) at the same time-step of LSTM. Instead, we factor the J-dimensional distribution of joint configurations $y(x)$ into a product of one-dimensional distributions, in this order: base, shoulder, elbow, ..., and gripper. The probability distribution in this approach is modeled using a linear combination of Gaussian kernel functions of the form

$$p(y|x) = \sum_{i=1}^m \alpha_i(x) g_i(y|x) \quad (1)$$

in which $\alpha_i(x)$ is the mixing coefficient, $g_i(y|x)$ is a multivariate Gaussian, and m is the number of kernels. At each time-step, the output is $y = y_t^j$, the current joint to be predicted and input is $x = \{x_1^1 \dots x_t^{<j}\}$, the encoded history of observations and predictions of the network before predicting the current joint. The Gaussian kernel is of the form

$$g(y|x) = \frac{1}{(2\pi)^{c/2} \sigma_i(x)} \exp \left\{ -\frac{\|y - \mu_i(x)\|^2}{2\sigma_i(x)^2} \right\} \quad (2)$$

where the vector $\mu_i(x)$ is the center of i th kernel. We do not calculate the full covariance matrices for each component, since this form of Gaussian mixture model is general enough to approximate any density function [25].

In the network architecture, we use skip connections from the input to all LSTM layers [11]. Then the output of all LSTM layers are concatenated together and then fully connected to another layer with width $3 \times m$. This layer contains m neurons for $\mu_i(x)$, m neurons for $\sigma_i(x)$, and another m

neurons for $\alpha_i(x)$. To satisfy the constraint $\sum_{i=1}^m \alpha_i(x) = 1$, the corresponding neurons are passed through a softmax function. The neurons corresponding to the variances $\sigma_i(x)$ are passed through an exponential function and the neurons corresponding to the means $\mu_i(x)$ are used without any further changes. Finally, we can define the error in terms of negative logarithm likelihood

$$E = -\ln \left\{ \sum_{i=1}^m \alpha_i(x) g_i(y|x) \right\} \quad (3)$$

Details of the implementation can be found in Appendix A

3.4 Executing the Policy at Test Time

During the test time, the trained neural network controller generates robot joint commands in a loop by observing the environment. The LSTM predicts each joint one by one and when the predictions of all the joints are available, the robot takes an action, and another image is recorded and fed into the controller. As we mentioned before, the user occasionally makes mistakes while demonstrating the task. However, it is desired that the robot does not repeat those mistakes. We can reduce the rate of mistakes by introducing some bias towards higher probability areas of the distribution while sampling from the probability distribution [11]. While sampling, we use the new mixing coefficient

$$\alpha_i(x) = \frac{\exp(\alpha_i(x)(1+b))}{\exp(\sum_{i=1}^m \alpha_i(x)(1+b))} \quad (4)$$

and standard deviation

$$\sigma_i(x) = \exp(\sigma_i(x)(1+b)) \quad (5)$$

where bias parameter b is a real number between 0 to 10. When $b = 0$, there is no bias while $b = 10$ introduces the maximum bias where only a point with maximum probability is chosen. We found $b = 1$ to work well in our experiments.

3.5 Why this Architecture?

Why predicting the entire probability distribution? Many robotics manipulation tasks can be solved in more than one way, and often the same human chooses randomly between the possible solutions. One approach would be to predict a deterministic joint command and use mean squared error to minimize the error between the predicted command and the command demonstrated by the user. In this approach, if there are multiple solutions demonstrated by the user, the network will learn to predict the average of these commands. However, averaging between multiple solutions is usually not a correct solution. For instance, the robot arm might avoid an object from the left or from the right, but the average of these solutions is a collision with the object. Our approach models the entire multimodal probability distribution of solutions and samples its solution from this space.

Why use recurrent neural networks? As shown above, humans might choose different solutions to a manipulation problem, but once decided, they need to stick to the chosen solution - they cannot choose between the avoid to the left or avoid to the right strategy at each time step. Using recurrent networks helps the robot to remember and stick to a particular strategy similar to humans. In addition, in many manipulation tasks a single input image is not enough for predicting the next action. For instance, sometimes the human demonstrator stops for a couple of time-steps to make sure the gripper is in the right place before grasping an object. In this case, a single image cannot help in deciding whether to wait for another time-step or continue. The model needs to remember and count the number of time-steps that it has been waiting before closing the gripper.

Another reason for using a recurrent neural network is that there will be timesteps where the model will fail to extract enough information from the current input to decide on what to do next. For instance, the manipulation object might be occluded or not encoded correctly due to the imperfection of the visual encoder. The LSTM recurrent neural networks are able to store this information and the controller can continue to act based on the network's memory until it regains the sight of the object.

Why autoregressive density estimator? By using this density estimator, we condition the prediction of each joint on the prediction of previous joints. Let us consider a situation in which an object is about to be grasped. The network needs to predict whether the gripper should be closed or not in the

next time-step. If we do not condition the prediction of gripper on the prediction of other joints in the current time-step, the gripper might be closed before the end-effector is in a good grasping angle. Therefore, the grasp will fail. This idea of modeling the joint probability distribution of outputs by casting it as a product of conditional distributions is used in Pixel RNNs [27], Neural Autoregressive Distribution Estimator (NADE) [19], and fully visible neural networks [26, 4].

4 Experiments

In order to evaluate our method, we consider several related manipulation tasks that are frequent components of ADLs found in assistive robotics. A 6-axis Lynxmotion AL5D robot with a two-finger gripper is used to perform the tasks. The entire setup, including the arm, the camera, the Leap Motion and Playstation controllers used for demonstration, costs about 500 USD, making it affordable and accessible. We plan to release our code upon acceptance, allowing anyone to experiment with our system.

4.1 Manipulation Tasks

In all of the following tasks the objects are placed in a random position and orientation within the reachability range of the robot arm. One of the challenges is that all the objects might get partially or completely occluded by the robot arm. In addition, because of the difficulty of the tasks and also the teleoperation method, the user often makes mistakes and tries again.

Task 1. In this task, the robot picks up a small bubble wrap and puts it into a small plate. This task is challenging since the robot needs to be very accurate while picking up the thin and deformable bubble wrap that often gets completely occluded by the arm during the grasp. If the bubble wrap is placed inside the plate, we count it as a success.

Task 2. In this task, the robot must push a round plate to a specified area on the left side of its workspace. This task is challenging because the robot needs to accurately detect the position of the plate and push at a point that moves the plate in the desired direction. In addition, if the plate ended up moving to an unexpected direction, the arm must push from a completely different contact point to fix the problem. If the plate is placed within an area with the radius of 2cm larger than the radius of the plate, we count it a success.

Task 3. In this task, the robot pushes a large box, which is too large to be grasped, and places it close to its base with a certain position and orientation. This task is challenging because the robot needs to adjust the orientation of the box within a 20° error range and the position of the box within an area that is 2cm wider than the box in each direction. So, if for instance the robot pushes the box further to the right such that it exits the target area, the arm has to circle around the box without colliding with it to push it from the other side.

Task 4. In this task, water pump pliers are placed on the desk in the open position. The robot needs to close the pliers and orient them parallel to the borders of the table. In this task the convolutional layers need to detect the thin handles of the pliers so that the LSTM can decide where to push to accomplish the task. The pliers needs to be completely closed while 10° of error is acceptable for its final orientation. Note that in this task the initial orientation of the pliers is in a way that the handles are closer than its head to the base of the robot arm.

Task 5. In this task, the robot needs to pick up a towel and rub a small screwdriver box to clean it. We count the task as a success if the robot successfully picks up the towel, rubs the whole screwdriver box at least one time, and places the towel back on the table. (The quality of the cleaning was not considered in evaluating the success of this task).

4.2 Compared Methods

In this part we compare different variations of the proposed method to see which one works best. The compared approaches are as follows:

Single-task. The network architecture is as explained in Figure 2. However, we train it on the data of a single task. This means that the one-hot task selector vector will not be used. In addition, all the joints are predicted at the same time, therefore, it is not an autoregressive estimator.

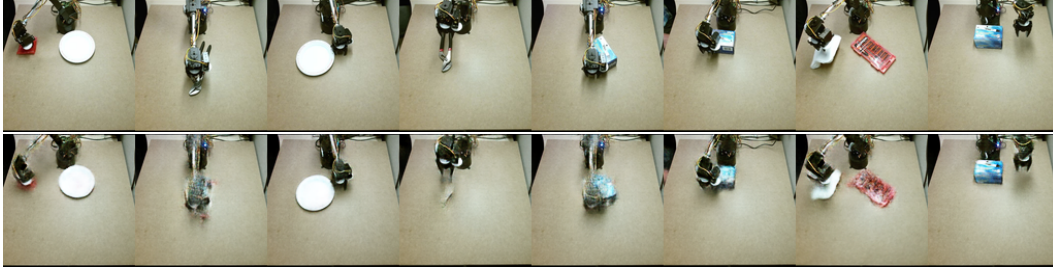


Figure 3: Original input images to the network are shown on the top row. For each original image, the corresponding reconstructed image by the autoencoder is shown in the bottom row.

Method	Task 1	Task 2	Task 3	Task 4	Task 5
Single-task	36%	16%	44%	16%	8%
Multi-task	16%	20%	52%	64%	20%
Multi-task autoregressive (no reconstruction)	12%	72%	56%	48%	16%
Multi-task autoregressive	76%	80%	88%	76%	88%

Table 1: Performance comparison of different methods. The numbers are the percentile rate of successfully accomplishing the tasks.

Multi-task. This method is the same as single-task method, however, we train it on the data of all tasks and then we use the one-hot task selector vector to decide which task should be performed.

Multi-task autoregressive (no reconstruction). this approach utilized the autoregressive estimator and is trained on the data of all tasks. However, we exclude the VAE/GAN that adds the reconstruction to the error signal. This way we can see if the reconstruction part of the network really helps in improving the learning.

Multi-task autoregressive. this is the main approach that contains the autoregressive estimator and reconstruction error, and also is trained on the data of all tasks.

4.3 Results

Video clips of the demonstration process and of the robot autonomously performing the five tasks can be watched on our online account¹. Note that to get an accurate impression of the results, it is strongly recommended that the reader watches the accompanying videos.

First we show how the autoencoder can reconstruct the input images in Figure 3. This shows that all the objects and the arm itself are captured and encoded quite well in most cases. Therefore, the LSTM has useful information to generate a trajectory to accomplish the task.

In order to quantitatively evaluate the performance of our method, we allow the robot to try each task 25 times. If it cannot accomplish the task in a limited time (45 seconds for task 1, 60 seconds for tasks 2-4, and 75 seconds for task 5), we count the try as a failure, place the objects in a new random pose and repeat the experiment. Note that we do not stop the controller while we are resetting the experiment since this has also been the case during the demonstrations. It is interesting that the robot learned to go to the default state when it finishes the task since this was the preference of the user while demonstrating. Table 1 shows the difference in performance of compared methods.

Now we describe and analyze the performance of each method:

Single-task. Training this network is difficult since it overfits very easily. Our attempts to avoid or delay overfitting by increasing the dropout ratio or making the network smaller did not improve the results. The proposed model is very powerful and it does not have any assumption about the task or the shape of objects that are involved in each task. This is good since we can train the model

¹https://www.youtube.com/playlist?list=PL5i33tEH-MHfrXjj_Nek10jyqgdJomg_a

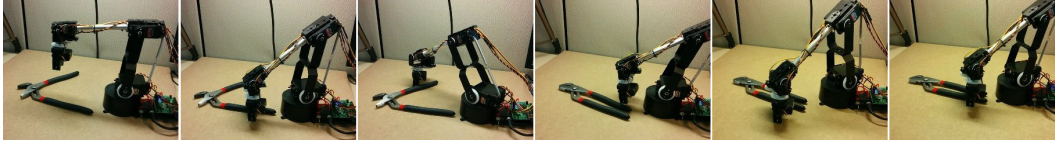


Figure 4: The robot makes mistakes but fixes them. Sequence of images from left to right shows the performance of the robot. The task here is to close and orient the water pump pliers. When the pliers are pushed more than expected, the robot turns around and pushes the other side to move the pliers back to the desired orientation.

on a wide variety of tasks. However, we need large number of demonstrations to successfully learn a single task. The controller trained using this approach generates some movements that are often similar to the demonstrations. However, they are not accurate enough to finish the task most of the time. Sometimes abrupt movements send the objects to an unseen configuration or out of the reachability range of the robot.

Multi-task. This model works much better than the previous model since there is more data that leads to more stable training. The common patterns among different tasks can be well captured since there is enough data from different tasks. For instance, consider a time when the gripper is close to an object (bubble wrap or paper towel) and the model needs to decide if the gripper should be closed or not in the next time-step. There is large variance in the data of one task due to imperfect demonstrations and model. However, when grasping is an element of two different tasks, the data for this pattern is doubled which leads to a better prediction.

Multi-task autoregressive (no reconstruction). The vision part of this model is not well trained especially in the tasks where the objects are smaller or occluded more often. This is probably because the training examples are not enough to train the visual feature extractor of the controller. In the tasks where the objects are larger and vision is the easy part (e.g., task 3), the robot achieves acceptable results.

Multi-task autoregressive. This model achieves the best results compared to the rest. Our observation was that this model generates very smooth trajectories that take a reasonable path in different situations. Interestingly, this model has also learned to fix its own mistakes most of the time. Take a look at Figure 4 for an example of mistake-fixing behaviour. To understand why this model works better consider the following example. When the gripper is close to an object that needs to be grabbed, the event for closing the gripper might be triggered. In this model the uncertainty is diminished since we delay the prediction of the gripper to the future when all other joints are already known. Therefore, the model knows better if the gripper will have a good contact with the object for a more stable grasp or not. Hence, the chances of a more successful grasp increases.

5 Conclusions

In this paper we proposed an approach to multi-task learning of manipulation tasks from user demonstrations. The approach takes as input images of the environment and outputs the next joint configuration of the robot. We showed that this approach works well on a low cost robot on basic manipulation tasks such as pushing and grasping. We also showed that the method can plan for longer tasks such as cleaning a small object using a towel. The proposed method is more sample-efficient compared to the single-task approach. This is because there is more data from the common patterns in different tasks that help the network to learn them easier.

While we demonstrate our approach on a set of five tasks, our results strongly suggest that the path toward robotic manipulators that can execute a wide variety of tasks lies in multi-task learning. Since our setup is inexpensive and accessible, we might imagine that, in the future, a large number of end-users could specify their own tasks to their own robots using our method. As more and more task demonstration data is collected, it can be used to train a single multi-task network. We expect that, as more tasks are added to the dataset, the number of individual demonstrations needed for each individual task will decrease, such that only a handful of additional demonstrations might be needed to allow the robot to perform each new behavior. Exploring this possibility is an exciting and promising direction for future work.

References

- [1] P. Abbeel, A. Coates, and A. Y. Ng. Autonomous helicopter aerobatics through apprenticeship learning. *International Journal of Robotics Research (IJRR)*, 2010.
- [2] P. Agrawal, A. Nair, P. Abbeel, J. Malik, and S. Levine. Learning to poke by poking: Experiential learning of intuitive physics. *arXiv preprint arXiv:1606.07419*, 2016.
- [3] J. L. Ba, J. R. Kiros, and G. E. Hinton. Layer normalization. *arXiv preprint arXiv:1607.06450*, 2016.
- [4] Y. Bengio and S. Bengio. Modeling high-dimensional discrete data with multi-layer neural networks. In *Advances in neural information processing systems (NIPS)*, volume 99, pages 400–406, 1999.
- [5] C. M. Bishop. Mixture density networks. *Technical Report*, 1994.
- [6] S. Calinon, F. D’halluin, E. L. Sauser, D. G. Caldwell, and A. G. Billard. Learning and reproduction of gestures by imitation. *IEEE Robotics & Automation Magazine*, 17(2):44–54, 2010.
- [7] R. Caruana. Learning many related tasks at the same time with backpropagation. *Advances in neural information processing systems*, pages 657–664, 1995.
- [8] M. P. Deisenroth, P. Englert, J. Peters, and D. Fox. Multi-task policy search for robotics. In *IEEE International Conference on Robotics and Automation (ICRA)*, pages 3876–3881. IEEE, 2014.
- [9] C. Devin, A. Gupta, T. Darrell, P. Abbeel, and S. Levine. Learning modular neural network policies for multi-task and multi-robot transfer. *arXiv preprint arXiv:1609.07088*, 2016.
- [10] I. Goodfellow, J. Pouget-Abadie, M. Mirza, B. Xu, D. Warde-Farley, S. Ozair, A. Courville, and Y. Bengio. Generative adversarial nets. In *Advances in neural information processing systems*, pages 2672–2680, 2014.
- [11] A. Graves. Generating sequences with recurrent neural networks. *arXiv preprint arXiv:1308.0850*, 2013.
- [12] S. Hochreiter and J. Schmidhuber. Long short-term memory. *Neural computation*, 9(8):1735–1780, 1997.
- [13] S. Ioffe and C. Szegedy. Batch normalization: Accelerating deep network training by reducing internal covariate shift. *arXiv preprint arXiv:1502.03167*, 2015.
- [14] D. Kingma and J. Ba. Adam: A method for stochastic optimization. *arXiv preprint arXiv:1412.6980*, 2014.
- [15] D. P. Kingma and M. Welling. Auto-encoding variational bayes. *arXiv preprint arXiv:1312.6114*, 2013.
- [16] D. P. Kingma, S. Mohamed, D. J. Rezende, and M. Welling. Semi-supervised learning with deep generative models. In *Advances in Neural Information Processing Systems*, pages 3581–3589, 2014.
- [17] J. Kober, J. A. Bagnell, and J. Peters. Reinforcement learning in robotics: A survey. *The International Journal of Robotics Research*, 32(11):1238–1274, 2013.
- [18] G. Konidaris and A. Barto. Autonomous shaping: Knowledge transfer in reinforcement learning. In *Proceedings of the 23rd international conference on Machine learning*, pages 489–496. ACM, 2006.
- [19] H. Larochelle and I. Murray. The neural autoregressive distribution estimator. In *AISTATS*, volume 1, page 2, 2011.

- [20] A. B. L. Larsen, S. K. Sønderby, H. Larochelle, and O. Winther. Autoencoding beyond pixels using a learned similarity metric. In *International Conference on Machine Learning*, pages 1558–1566, 2016.
- [21] S. Levine, C. Finn, T. Darrell, and P. Abbeel. End-to-end training of deep visuomotor policies. *Journal of Machine Learning Research*, 17(39):1–40, 2016.
- [22] S. Levine, P. Pastor, A. Krizhevsky, and D. Quillen. Learning hand-eye coordination for robotic grasping with deep learning and large-scale data collection. *arXiv preprint arXiv:1603.02199*, 2016.
- [23] T. P. Lillicrap, J. J. Hunt, A. Pritzel, N. Heess, T. Erez, Y. Tassa, D. Silver, and D. Wierstra. Continuous control with deep reinforcement learning. *arXiv preprint arXiv:1509.02971*, 2015.
- [24] M. G. Madden and T. Howley. Transfer of experience between reinforcement learning environments with progressive difficulty. *Artificial Intelligence Review*, 21(3):375–398, 2004.
- [25] G. J. McLachlan and K. E. Basford. Mixture models. inference and applications to clustering. *Statistics: Textbooks and Monographs, New York: Dekker*, 1, 1988.
- [26] R. M. Neal. Connectionist learning of belief networks. *Artificial intelligence*, 56(1):71–113, 1992.
- [27] A. V. d. Oord, N. Kalchbrenner, and K. Kavukcuoglu. Pixel recurrent neural networks. In *International Conference on Machine Learning*, pages 1747–1756, 2016.
- [28] P. Pastor, H. Hoffmann, T. Asfour, and S. Schaal. Learning and generalization of motor skills by learning from demonstration. In *IEEE International Conference on Robotics and Automation (ICRA)*, pages 763–768, 2009.
- [29] J. Peters and S. Schaal. Reinforcement learning of motor skills with policy gradients. *Neural networks*, 21(4):682–697, 2008.
- [30] L. Pinto and A. Gupta. Supersizing self-supervision: Learning to grasp from 50k tries and 700 robot hours. In *IEEE International Conference on Robotics and Automation (ICRA)*, pages 763–768, 2016.
- [31] L. Pinto and A. Gupta. Learning to push by grasping: Using multiple tasks for effective learning. *arXiv preprint arXiv:1609.09025*, 2016.
- [32] R. Rahmatizadeh, P. Abolghasemi, A. Behal, and L. Bölöni. Learning real manipulation tasks from virtual demonstrations using LSTM. *arXiv preprint arXiv:1603.03833*, 2016.
- [33] J. Ramon, K. Driessens, and T. Croonenborghs. Transfer learning in reinforcement learning problems through partial policy recycling. In *European Conference on Machine Learning*, pages 699–707. Springer, 2007.
- [34] N. Srivastava, G. Hinton, A. Krizhevsky, I. Sutskever, and R. Salakhutdinov. Dropout: A simple way to prevent neural networks from overfitting. *The Journal of Machine Learning Research*, 15(1):1929–1958, 2014.
- [35] J. Sung, S. H. Jin, and A. Saxena. Robobarista: Object part-based transfer of manipulation trajectories from crowd-sourcing in 3d pointclouds. In *International Symposium on Robotics Research (ISRR)*, 2015.
- [36] I. Sutskever, O. Vinyals, and Q. V. Le. Sequence to sequence learning with neural networks. In *Advances in neural information processing systems (NIPS)*, pages 3104–3112, 2014.
- [37] M. E. Taylor and P. Stone. Transfer learning for reinforcement learning domains: A survey. *Journal of Machine Learning Research*, 10(Jul):1633–1685, 2009.
- [38] T. Tieleman and G. Hinton. Lecture 6.5-rmsprop: Divide the gradient by a running average of its recent magnitude. *COURSERA: Neural Networks for Machine Learning*, 4, 2012.

A Implementation Details

We ask the user to demonstrate some related manipulation tasks with a two finger robotic arm. During the demonstration we record the commands sent to the robot as well as 128×128 RGB images of the scene at a frequency of 33Hz. Then we down-sample the trajectories to reach a frequency of 4Hz. This way we create redundant trajectories with different starting point offsets [32]. For instance, if we have a high frequency trajectory $\{t_1, t_2, \dots\}$, after down-sampling it by a factor of 8, we will have 8 trajectories $\{t_1, t_9, t_{17}, \dots\}$, $\{t_2, t_{10}, t_{18}, \dots\}$, etc. We found this data augmentation technique to be useful in regularizing the network.

We collected 3 hours of demonstrations for each task, which is equivalent to 909, 495, 431, 428, 398 times completion of each task for tasks 1-5, respectively. These comparatively high number of demonstration counts for a reasonable time frame of demonstration illustrate how a convenient and intuitive demonstration system can improve the data collection. We used 80% of this data for training and kept the remaining 20% for validation.

Except the latent space size that is set to 256, other parameters of the autoencoder are set and initialized according to the original paper [20]. All other parameters including LSTM parameters are initialized uniformly between -0.08 to 0.08 following the recommendation by [36]. Each LSTM layer has 100 memory cells and is connected to a mixture of Gaussians with 50 components. We first unroll and train the network using sequences of 5 time-steps and batch size of 100 examples for 5 epochs. Then for faster training, we train only the LSTM layers using sequences of 50 time-steps and mini-batches of size 128 for 2000 epochs. In the first phase of training, Adam optimizer [14] is used while for fine tuning LSTM layers, RMSProp [38] with initial learning rate of 0.005 and decay of 0.999. In order to overcome the exploding gradients problem, the gradients are clipped in the range [-1, 1]. During the fine-tuning, the learning rate is decreased by a factor of 2 in every 100 epochs.